UCLA
UCLA Previously Published Works

Title

Effects of renal sympathetic denervation on the stellate ganglion and brain stem in dogs

Authors

Tsai, Wei-Chung
Chan, Yi-Hsin
Chinda, Kroekkiat
et al.

Effects of Renal Sympathetic Denervation on the Stellate Ganglion and the Brain Stem in Dogs

Wei-Chung Tsai, MD[1,2], **Yi-Hsin Chan, MD**[1,3], **Kroekkiat Chinda, DVM, PhD**[1,4], **Zhenhui Chen, PhD**[1], **Jheel Patel, BS**[1], **Changyu Shen, PhD**[5], **Ye Zhao, MD**[1,6], **Zhaolei Jiang, MD**[1,7], **Yuan Yuan, MD**[1,7], **Michael Ye, BA**[1], **Lan S. Chen, MD**[8], **Amanda A. Riley, BA**[9], **Scott A. Persohn, BS**[9], **Paul R. Territo, PhD**[9], **Thomas H. Everett IV, PhD**[1], **Shien-Fong Lin, PhD**[1,10], **Harry V. Vinters, MD**[11], **Michael C. Fishbein, MD**[11], and **Peng-Sheng Chen, MD**[1]

[1]The Krannert Institute of Cardiology and Division of Cardiology, Department of Medicine, Indiana University School of Medicine, Indianapolis, IN, where the work was performed [2]Division of Cardiology, Department of Internal Medicine, Kaohsiung Medical University Hospital, Kaohsiung Medical University, Kaohsiung, Taiwan [3]The Cardiovascular Department, Chang Gung Memorial Hospital, Linkou, Taoyuan, Taiwan [4]Department of Physiology, Faculty of Medical Science, Naresuan University, Phitsanulok, Thailand [5]The Department of Biostatistics, Indiana University School of Medicine and the Fairbanks School of Public Health, Indianapolis, IN [6]Department of Cardiac Surgery, the First Affiliated Hospital of China Medical University, China [7]Department of Cardiothoracic Surgery, Xinhua Hospital, Shanghai Jiaotong University School of Medicine [8]Department of Neurology, Indiana University School of Medicine [9]Department of Radiology and Imaging Sciences, Indiana University, School of Medicine [10]Institute of Biomedical Engineering, National Chiao-Tung University, Hsin-Chu, Taiwan [11]The Department of Pathology and Laboratory Medicine, David Geffen School of Medicine at UCLA

Abstract

Background—Renal sympathetic denervation (RD) is a promising method of neuromodulation for the management of cardiac arrhythmia.

Objective—We tested the hypothesis that RD is antiarrhythmic in ambulatory dogs because it reduces the stellate ganglion nerve activity (SGNA) by remodeling the stellate ganglion (SG) and brain stem.

Methods—We implanted a radiotransmitter to record SGNA and electrocardiogram in 9 ambulatory dogs for 2 weeks, followed by a 2nd surgery for RD and 2 months SGNA recording.

Correspondence: Peng-Sheng Chen, 1800 N. Capitol Ave, Suite E475, Indianapolis, IN, 46202-1228 Telephone number: (317) 274-0909, Fax: (317) 962-0588, chenpp@iu.edu.

Cell death was probed by terminal deoxynucleotidyl transferase dUTP nick end labeling (TUNEL) assay.

Results—Integrated SGNA at baseline, 1 and 2 months after RD were 14.0±4.0, 9.3±2.8 and 9.6±2.0 µV, respectively (p=0.042). The SG from RD but not normal control (N=5) dogs showed confluent damage. An average of 41±10% and 40±16% of ganglion cells in the left and right SG, respectively, were TUNEL-positive in RD dogs compared with 0% in controls dogs (p= 0.005 for both). Left and right SG from RD dogs had more tyrosine hydroxylase-negative ganglion cells than left SG of control dogs (p= 0.028 and 0.047 respectively). Extensive TUNEL positive neurons and glial cells were also noted in the medulla, associated with strongly positive glial fibrillary acidic protein staining. The distribution was heterogeneous, with more cell death in the medial than lateral aspects of the medulla.

Conclusion—Bilateral RD caused significant central and peripheral sympathetic nerve remodeling and reduced SGNA in ambulatory dogs. These findings may in part explain the antiarrhythmic effects of RD.

Keywords

nervous system; sympathetic; catheter ablation; arrhythmia; neuromodulation

Recent studies showed that neuromodulation may be effective in controlling cardiac arrhythmias.[1, 2] Renal sympathetic denervation (RD) is one of the promising methods of neuromodulation in arrhythmia control.[3] RD was reported to decrease norepinephrine spillover and muscle sympathetic-nerve activity[4, 5] and may be useful in controlling electrical storm and atrial fibrillation.[6, 7] In the latter studies, the effects of RD persisted for weeks or months after a single procedure. The mechanisms of persistent antiarrhythmic effects remain unclear. Huang et al[8] showed that stimulating the sympathetic nerves around the renal artery may enhance the function of the left stellate ganglion (LSG). However, no studies directly measured the stellate ganglion nerve activity (SGNA) in ambulatory animals before and after RD to determine if RD reduces sympathetic outflow. The purpose of the present study was to perform SGNA recording in ambulatory dogs and histological studies of the SG and brain stem to test the hypothesis that RD causes SG and brain stem remodeling and reduces SGNA.

Methods

The study protocols were approved by the Institutional Animal Care and Use Committee. A detailed method section is included in an Online Supplement. Nine dogs were used as the experimental group for RD followed by SGNA, subcutaneous electrocardiogram (ECG) and blood pressure (BP) recording over a 2-month period using an implanted radiotransmitter. The SG and brain stem were harvested for histological analyses. Five normal dogs were used for histological controls. The SG were stained with antibodies against tyrosine hydroxylase (TH), growth-associated protein 43 (GAP43), hematoxylin and eosin and Masson's trichrome. Cell death was probed by terminal deoxynucleotidyl transferase dUTP nick end labeling (TUNEL) assay. The TUNEL assay was also used to determine the cell death in medulla. To detect the reactive astrocytosis, we performed glial fibrillary acidic protein

(GFAP) stains in medulla.[9, 10] An additional 2 dogs underwent brain stem ^{18}F-2-Fluoro-2-deoxyglucose (^{18}F-FDG) positron emission tomography–magnetic resonance imaging (PET/MRI) before and after RD to detect functional changes of the brain stem.

Results

Renal Sympathetic Denervation

Up to 6 ablations at 8 watts for 120 s each were successfully performed in bilateral renal arteries in 6 of 9 dogs. The results of these 6 dogs were used for statistical analyses. Right unilateral RD was performed in 3 dogs that had small (<2 mm diameter) dual left side renal arteries. There was luminal indentation after RF energy application when the vessel diameter was less than 4mm, but no significant renal arterial stenosis was found in any dog. Figure 1 shows examples of renal angiogram before, during and after RD.

Nerve Activities and Blood Pressure Recording

Table 1 shows nerve activities, RR interval and BP recorded by the radiotransmitter. The 24-hr average SGNA (aSGNA) at 1 and 2 months after RD were significantly reduced as compared with baseline (p= 0.042). The 24-hr average integrate vagal nerve activity (iVNA) at 1 month and 2 months after RD was non-significantly reduced from baseline (p= 0.115). There were no significant changes of 24-hr average RR interval, systolic BP and diastolic BP at 1 and 2 months after RD. The plasma norepinephrine level was 0.146 (CI, 0.077–0.215) ng/mL at baseline and 0.098 (0.041–0.155) ng/mL at 2 months after RD (p= 0.500).

The heart rate variability (HRV) and baroreflex sensitivity (BRS) were also performed to see the autonomic balance before and after RD. The standard deviation of normal to normal R-R intervals (SDNN) before and after RD were 295 (CI, 259–330) ms and 306 (CI, 241–371) ms respectively; the low frequency to high frequency ratio (LF/HF) before and after RD were 0.73 (CI, 0.38–1.09) and 0.56 (CI, 0.25–0.87) respectively; the BRS phase-rectified signal averaging (BRSprsa) before and after RD were 10 (CI, 3–16) and 11 (CI, 5–16) ms/mmHg respectively. None of the above comparisons were statistically significant. These findings might be partially explained by our previous study[11] which showed that HRV parameters poorly correlates with SGNA in ambulatory dogs.

Supplemental Figure 1A–B shows that these ambulatory dogs normally have paroxysmal atrial tachycardia (PAT) episodes, defined as an abrupt (> 50 bpm increment) increase or decrease in the heart rate, that persisted for at least 5 s, with a rate of > 150 bpm during the tachycardia. There were no ventricular arrhythmias. Among the 545 episodes of PATs analyzed, 543 (99.6%) episodes were preceded by SGNA. The patterns of SGNA discharges[12] were high amplitude spike discharges in 180 episodes (33%) and low amplitude burst discharges in 363 episodes (67%). The mean PAT episodes were 30 (CI, 19–41)/d, 14 (CI, 7–20)/d and 15 (CI, 7–22) times/d, respectively, at baseline, 1 and 2 months after RD (C) (p= 0.009). The duration of PAT were 269 (CI, 134–403) s/d, 118 (CI, 65–172) s/d and 131 (CI, 60–202) s/d, respectively, at baseline, and 1 and 2 months after RD (D) (p=0.115). RD did not change the AT rate. 545 AT episodes in 9 dogs. Supplemental Figures 1C–E illustrate these changes.

Histological Findings of Renal Nerve After Renal Sympathetic Denervation

Figure 2 shows typical examples of renal sympathetic nerve damage induced by RD. Panel **A** shows a hematoxylin-eosin stained section demonstrating normal media and injured media of the renal artery, with traumatic neuroma formation (arrowhead) with a region of nerve sprouting. Panel **B** shows neointima formation in the injured media region of the same renal artery. The traumatic neuroma (arrowhead) in Panel **A** is shown at higher magnification in Figures 2C. There were pyknotic nuclei and vacuolization of cytoplasm in the cells within the traumatic neuroma. The perineurium region shows nerve sprouting. Tyrosine hydroxylase (TH) staining (Figures 2D) showed TH-positive nerve structure in the traumatic neuroma.

Stellate Ganglion Remodeling

The SG from RD showed large regions of injury (Figure 3A). Multiple ganglion cells showed pyknotic nuclei and contracted cytoplasm (black arrow) in the Masson's trichrome stained sections (Figure 3A, B). These changes were not observed in any SG from the normal dogs. TH staining (Figure 3C and 3D) of the same region shows the presence of multiple TH-negative cells (arrowhead) in the region. The morphology of the TH-negative cells (pyknotic nucleus and contracted cytoplasm) suggested cell death. To further confirm cell death, we probed the ganglion cells with terminal deoxynucleotidyl transferase dUTP nick end labeling (TUNEL) staining (Figures 3E and 3F). There were multiple TUNEL positive ganglion cells in that region, confirming the presence of cell death. In contrast, none of the ganglion cells from normal dogs were TUNEL positive. The Confocal image (Figure 4A) showed TUNEL-positive (green) nuclei in both TH-positive (red) and TH-negative (yellow arrow) ganglion cells. TH-positive and TUNEL negative ganglion cells were observed in control SG (yellow arrowhead). An average of 41% (CI, 32%–49%) and 40% (CI, 26%–54%) of ganglion cells in the LSG and right SG (RSG), respectively, of the RD dogs were TUNEL-positive. In comparison, none of the ganglion cells in control dogs were TUNEL positive (p= 0.005; Figure 4B). TH-negative ganglion cells accounted for 19% (CI, 14%–24%) and 15% (CI, 13%–18%) of the cells in the LSG and the RSG, respectively. They were significantly more than that of the controls (10%; CI, 6%–13%, p= 0.028 and 0.047 respectively; Figure 4C). In two dogs with unilateral right side RD, the LSG showed 0% and 28% of TUNEL positivity, respectively. The density of GAP43 immunoreactivity in the LSG and RSG were 7616.1 (CI, 3089.7–12142.5) $\mu m^2/mm^2$ and 7205.1 (CI, 1808.2–12601.9) $\mu m^2/mm^2$, respectively, in the RD group. The density of GAP43 immunoreactivity in the LSG was 7500.7 (CI, 1250.4–13751.1) $\mu m^2/mm^2$ in the control group. There were no difference in GAP43 immunoreactivity between RD-LSG, RD-RSG and control dogs (p= 0.917).

Remodeling in Brain stem

Figure 5A shows a TUNEL stained medulla at high level. This image was generated by combining multiple images taken from the confocal microscope. The red rectangle indicates part of "damaged zones", defined by regions in the brain stem with multiple TUNEL-positive cells. The white rectangle indicates part of "non-damaged zones" where TUNEL staining was negative. In all five levels of the brain stem, the TUNEL-positive cells were

heterogeneously distributed. Figure 5B shows a schematic of TUNEL-positivity. Dark blue crosses mark the damaged zones. Figure 5C and 5D show the high magnification view of red and white rectangles in Figure 5A, respectively. Filled arrowhead and arrow in Figure 5C indicate the TUNEL positive neuron and neuroglia, respectively. The TUNEL positive neuroglia were glial fibrillary acidic protein (GFAP) positive (red), suggesting strong glial cell reaction. The percentage of neurons that were TUNEL positive was much higher in damaged zones (54.8; CI, 42.1–67.5) than non-damaged zones (3.0; CI, −2.3–8.2, p=0.043). The percentage of glial cells that were TUNEL positive was much higher in damaged zones (35.1 CI, 22.4–47.9) than non-damaged zones (4.9; CI, 1.0–8.8, p=0.043) (Figure 5E). Supplemental Figure 2 shows the GFAP stain of damaged and non-damaged zones, respectively. Brown color indicates the GFAP positive glial cell. The densities of GFAP immunoreactivity are higher in the damaged zones than in non-damaged zones in the RD group (Supplemental Figure 2C). All layers of the brain stem showed similar heterogeneous distribution of the TUNEL and GFAP positivity. The following structures in brain stems from RD dogs showed positive stains: nuclei of raphe, nucleus solitaries and tract, medial and lateral reticular nuclei, medial lemniscus, vagal dorsal motor nucleus, nucleus ambiguous and commissural sensory nucleus of vagus. Most of the involved areas were relevant to the autonomic nervous system. Consistent with the histological results, PET/MRI showed reduced ^{18}F-FDG uptake at 1 week and 8 weeks after RD in both dogs studied (Supplemental Figures 3 and 4).

Discussion

We demonstrated in ambulatory canines that bilateral RD caused significant brain stem and bilateral SG remodeling, including neuronal cell death and active glial cell reaction at 8 weeks after the procedure. These changes were associated with reduced ^{18}F-FDG uptake in brain stem, left aSGNA and atrial tachyarrhythmia episodes. We propose that neural remodeling in the brain stem and SG may partially explain the antiarrhythmic effects of RD.

Connection between the Renal Sympathetic Nerve and the Stellate Ganglia

Trans-synaptic (transneuronal) degeneration is a phenomenon in the central and peripheral nervous system that may remain active both at the level of the insult and in the remote brain structures up to 1 year post-trauma.[13] These progressive changes may underlie some of the long-term functional consequences after initial injury. Figure 6 summarizes the various direct and indirect connections between renal sympathetic nerve and the SG based on the literature search. Meckler et al[14] showed that approximately 10% of bilateral renal sympathetic neurons in cats originated from the thoracic chain ganglia (stellate through T13). Because of the connections between these two structures, RD may directly result in retrograde cell death of the SG. In addition, application of fluorescent dyes in the renal nerves resulted in fluorescent labeling of the sympathetic cell bodies in paravertebral and prevertebral ganglia.[15–17] The latter nerve structures connected to the thoracic spinal cord.[18, 19] Because the sympathetic preganglionic neurons that projected to the SG were distributed in spinal segments T1-T10,[20] they had ample opportunities to interact with the preganglionic cells that connected indirectly with the sympathetic nerve fibers around the renal artery. There are other possible connections that might contribute to the transneuronal

degeneration. For example, the ganglion cells of renal afferent nerves were located in thoracic and lumbar spine dorsal root ganglia[21] that connect with the posterior and lateral hypothalamic nuclei and locus ceruleus in the brain stem.[22, 23] Because brain stem is also connected with the lateral horn of the thoracic spinal cord that innervates the SG,[24, 25] it is possible for the transneuronal degeneration to spread from the brain stem to the preganglionic sympathetic neurons in the lateral horn and reach the SG. Because transneuronal degeneration may remain active for prolonged periods of time, the effects of RD on arrhythmia control may persist for months after the procedure.

Renal Sympathetic Denervation and Paroxysmal Atrial Tachycardia

We[26] have previously reported that normal dogs may have spontaneous PAT episodes both at baseline and after rapid atrial pacing. These PAT episodes were preceded by the SGNA. Therefore, PAT episodes are relevant measures of neuromodulation procedures such as cryoablation of the SG[27] and vagal nerve stimulation (VNS).[28, 29] These findings are consistent with the results of the present study, which showed that RD suppressed PATs through SG damages.

Clinical Implications

Our study helps to provide a mechanistical basis of the antiarrhythmic effects of RD.[3] In addition, RD may be helpful in controlling other types of arrhythmias known to be controllable by SG ablation. Absence of BP effects have been observed in the present study and in previous clinical studies,[6, 30] suggesting that hypotension may not be a side effect of RD.

Study Limitations

Due to the limitation of the DSI transmitters, we were able to record only from the LSG and not both SG. However, because RSG was not accessed or recorded, the neural damage and cell death in the RSG cannot be attributed to the damage caused by the recording procedures. Second, we only recorded for 2 months after RD. It remains unclear if the effects of RD on SGNA can persist for > 2 months. Our dogs did not have hypertension, cardiomyopathy or sleep apnea. Therefore, the results of the present study do not rule out the possibility that RD is effective in BP control in pathological conditions. A recent study suggested that renal nerve stimulation can be used as an acute end point for RD.[31] However, we did not perform renal nerve stimulation during the procedure. We observed only an insignificant decrease in serum norepinephrine level, consistent with that reported by Linz et al.[32] These findings suggest that the serum norepinephrine levels may have limited sensitivity in detecting the changes of norepinephrine release in various organs. Finally, we do not have long term follow up information to study the possible complications of RD.

Conclusions

Bilateral RD reduced SGNA and is associated with significant SG and brain stem remodeling. RD is a promising method of reducing sympathetic outflow and may therefore be effective in controlling arrhythmias triggered by sympathetic nerve activities.

Supplementary Material

Refer to Web version on PubMed Central for supplementary material.

Acknowledgments

References

1. Chen PS, Chen LS, Fishbein MC, Lin SF, Nattel S. Role of the autonomic nervous system in atrial fibrillation: pathophysiology and therapy. Circ Res. 2014; 114:1500–1515. [PubMed: 24763467]

2. Priori SG, Blomstrom-Lundqvist C, Mazzanti A, et al. 2015 ESC Guidelines for the management of patients with ventricular arrhythmias and the prevention of sudden cardiac death. Eur Heart J. 2015; 36:2793–2867. [PubMed: 26320108]

3. Nammas W, Airaksinen JK, Paana T, Karjalainen PP. Renal sympathetic denervation for treatment of patients with atrial fibrillation: Reappraisal of the available evidence. Heart Rhythm. 2016

4. Schlaich MP, Sobotka PA, Krum H, Lambert E, Esler MD. Renal sympathetic-nerve ablation for uncontrolled hypertension. N Engl J Med. 2009; 361:932–934. [PubMed: 19710497]

5. Krum H, Schlaich M, Whitbourn R, Sobotka PA, Sadowski J, Bartus K, Kapelak B, Walton A, Sievert H, Thambar S, Abraham WT, Esler M. Catheter-based renal sympathetic denervation for resistant hypertension: a multicentre safety and proof-of-principle cohort study. Lancet. 2009; 373:1275–1281. [PubMed: 19332353]

6. Remo BF, Preminger M, Bradfield J, Mittal S, Boyle N, Gupta A, Shivkumar K, Steinberg JS, Dickfeld T. Safety and efficacy of renal denervation as a novel treatment of ventricular tachycardia storm in patients with cardiomyopathy. Heart Rhythm. 2014; 11:541–546. [PubMed: 24389229]

7. Pokushalov E, Romanov A, Corbucci G, Artyomenko S, Baranova V, Turov A, Shirokova N, Karaskov A, Mittal S, Steinberg JS. A randomized comparison of pulmonary vein isolation with versus without concomitant renal artery denervation in patients with refractory symptomatic atrial fibrillation and resistant hypertension. J Am Coll Cardiol. 2012; 60:1163–1170. [PubMed: 22958958]

8. Huang B, Yu L, Scherlag BJ, Wang S, He BO, Yang K, Liao KAI, Lu Z, He W, Zhang L, Po SS, Jiang H. Left Renal Nerves Stimulation Facilitates Ischemia-Induced Ventricular Arrhythmia by Increasing Nerve Activity of Left Stellate Ganglion. Journal of Cardiovascular Electrophysiology. 2014; 25:1249–1256. [PubMed: 25066536]

9. Sofroniew MV, Vinters HV. Astrocytes: biology and pathology. Acta Neuropathol. 2010; 119:7–35. [PubMed: 20012068]

10. Barres BA, Barde Y. Neuronal and glial cell biology. Curr Opin Neurobiol. 2000; 10:642–648. [PubMed: 11084327]

11. Chan YH, Tsai WC, Shen C, Han S, Chen LS, Lin SF, Chen PS. Subcutaneous nerve activity is more accurate than heart rate variability in estimating cardiac sympathetic tone in ambulatory dogs with myocardial infarction. Heart Rhythm. 2015; 12:1619–1627. [PubMed: 25778433]

12. Zhou S, Jung BC, Tan AY, Trang VQ, Gholmieh G, Han SW, Lin SF, Fishbein MC, Chen PS, Chen LS. Spontaneous stellate ganglion nerve activity and ventricular arrhythmia in a canine model of sudden death. Heart Rhythm. 2008; 5:131–139. [PubMed: 18055272]

13. Bramlett HM, Dietrich WD. Progressive damage after brain and spinal cord injury: pathomechanisms and treatment strategies. Prog Brain Res. 2007; 161:125–141. [PubMed: 17618974]

14. Meckler RL, Weaver LC. Comparison of the distributions of renal and splenic neurons in sympathetic ganglia. Journal of the Autonomic Nervous System. 1984; 11:189–200. [PubMed: 6491159]

15. Sripairojthikoon W, Wyss JM. Cells of origin of the sympathetic renal innervation in rat. Am J Physiol. 1987; 252:F957–963. [PubMed: 3591958]

16. Gattone VH 2nd, Marfurt CF, Dallie S. Extrinsic innervation of the rat kidney: a retrograde tracing study. Am J Physiol. 1986; 250:F189–196. [PubMed: 3753828]

17. Ferguson M, Ryan GB, Bell C. Localization of sympathetic and sensory neurons innervating the rat kidney. Journal of the Autonomic Nervous System. 1986; 16:279–288. [PubMed: 2427560]

18. Loukas M, Klaassen Z, Merbs W, Tubbs RS, Gielecki J, Zurada A. A review of the thoracic splanchnic nerves and celiac ganglia. Clinical Anatomy. 2010; 23:512–522. [PubMed: 20235178]

19. Strack AM, Sawyer WB, Hughes JH, Platt KB, Loewy AD. A general pattern of CNS innervation of the sympathetic outflow demonstrated by transneuronal pseudorabies viral infections. Brain Res. 1989; 491:156–162. [PubMed: 2569907]

20. Pilowsky P, Llewellyn-Smith IJ, Minson J, Chalmers J. Sympathetic preganglionic neurons in rabbit spinal cord that project to the stellate or the superior cervical ganglion. Brain Research. 1992; 577:181–188. [PubMed: 1606492]

21. Kuo DC, Nadelhaft I, Hisamitsu T, de Groat WC. Segmental distribution and central projectionsof renal afferent fibers in the cat studied by transganglionic transport of horseradish peroxidase. J Comp Neurol. 1983; 216:162–174. [PubMed: 6863600]

22. Moss, NG., Colindres, RE., Gottschalk, CW. Comprehensive Physiology. John Wiley & Sons, Inc; 2010. Neural Control of Renal Function.

23. Campese VM, Kogosov E. Renal afferent denervation prevents hypertension in rats with chronic renal failure. Hypertension. 1995; 25:878–882. [PubMed: 7721447]

24. Jansen ASP, Wessendorf MW, Loewy AD. Transneuronal labeling of CNS neuropeptide and monoamine neurons after pseudorabies virus injections into the stellate ganglion. Brain Res. 1995; 683:1–24. [PubMed: 7552333]

25. Jansen AS, Nguyen XV, Karpitskiy V, Mettenleiter TC, Loewy AD. Central command neurons of the sympathetic nervous system: basis of the fight-or-flight response. Science. 1995; 270:644–666. [PubMed: 7570024]

26. Choi EK, Shen MJ, Han S, Kim D, Hwang S, Sayfo S, Piccirillo G, Frick K, Fishbein MC, Hwang C, Lin SF, Chen PS. Intrinsic cardiac nerve activity and paroxysmal atrial tachyarrhythmia in ambulatory dogs. Circulation. 2010; 121:2615–2623. [PubMed: 20529998]

27. Tan AY, Zhou S, Ogawa M, Song J, Chu M, Li H, Fishbein MC, Lin SF, Chen LS, Chen PS. Neural mechanisms of paroxysmal atrial fibrillation and paroxysmal atrial tachycardia in ambulatory canines. Circulation. 2008; 118:916–925. [PubMed: 18697820]

28. Chinda K, Tsai WC, Chan YH, et al. Intermittent Left Cervical Vagal Nerve Stimulation Damages the Stellate Ganglia and Reduces Ventricular Rate During Sustained Atrial Fibrillation in Ambulatory Dogs. Heart Rhythm. 2016; 13:771–780. [PubMed: 26607063]

29. Shen MJ, Shinohara T, Park HW, et al. Continuous low-level vagus nerve stimulation reduces stellate ganglion nerve activity and paroxysmal atrial tachyarrhythmias in ambulatory canines. Circulation. 2011; 123:2204–2212. [PubMed: 21555706]

30. Bhatt DL, Kandzari DE, O'Neill WW, et al. A controlled trial of renal denervation for resistant hypertension. N Engl J Med. 2014; 370:1393–1401. [PubMed: 24678939]

31. de Jong MR, Adiyaman A, Gal P, et al. Renal Nerve Stimulation-Induced Blood Pressure Changes Predict Ambulatory Blood Pressure Response After Renal Denervation. Hypertension. 2016

32. Linz D, van Hunnik A, Hohl M, Mahfoud F, Wolf M, Neuberger HR, Casadei B, Reilly SN, Verheule S, Bohm M, Schotten U. Catheter-based renal denervation reduces atrial nerve sprouting and complexity of atrial fibrillation in goats. Circ Arrhythm Electrophysiol. 2015; 8:466–474. [PubMed: 25713217]
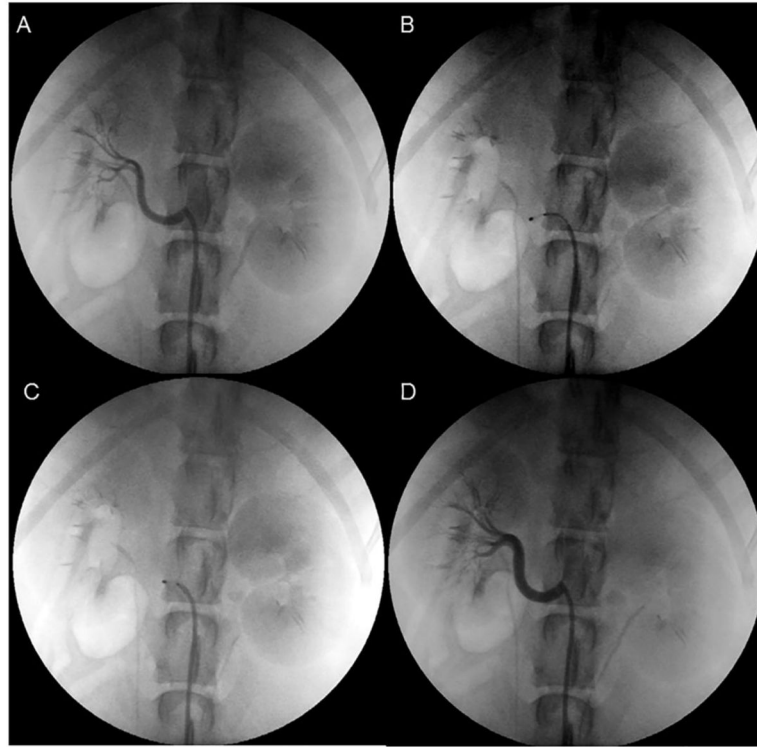
Figure 1. Angiograms of the renal artery
A was taken before ablation. **B** shows ablation catheter inserted into the main right renal artery, proximal to the renal artery bifurcation. **C** shows the ablation catheter was withdrawn gradually to the proximal segment of the right renal artery during the ablation procedure. **D** shows no evidence of significant spasm, thrombosis or stenosis after ablation.
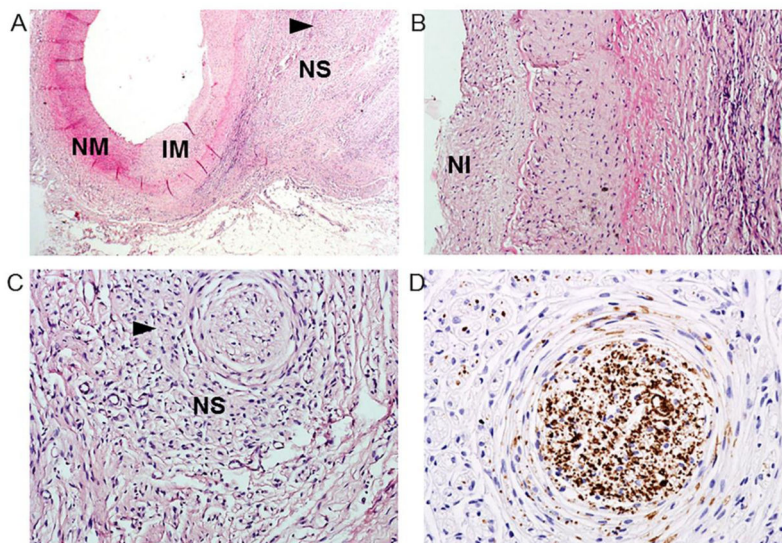
Figure 2. Typical examples of renal nerve injury induced by RD
A shows renal artery and sympathetic nerves in a dog with bilateral RD. H&E stain of the renal artery at low magnification **(A)** shows NM and IM of the renal artery, along with traumatic neuroma (arrowhead) in a region of NS. **B** shows a high magnification view of the renal artery wall with H&E staining. There was traumatic NI overlying the IM. **C** shows a high magnification view of the traumatic neuroma (arrowhead) with H&E staining. The traumatic neuroma cells contain pyknotic nuclei and vacuolization in endoneurium, with surrounding nerve sprouting. **D** shows TH staining (brown) of the traumatic neuroma at high magnification. (Panel A = 20X; B = 40X; C= 200X; D = 400X). H&E stain = Hematoxylin and eosin stain; IM = injured media; NI = neointima; NM = normal media; NS = nerve sprouting; RD = renal sympathetic denervation; TH = tyrosine hydroxylase.
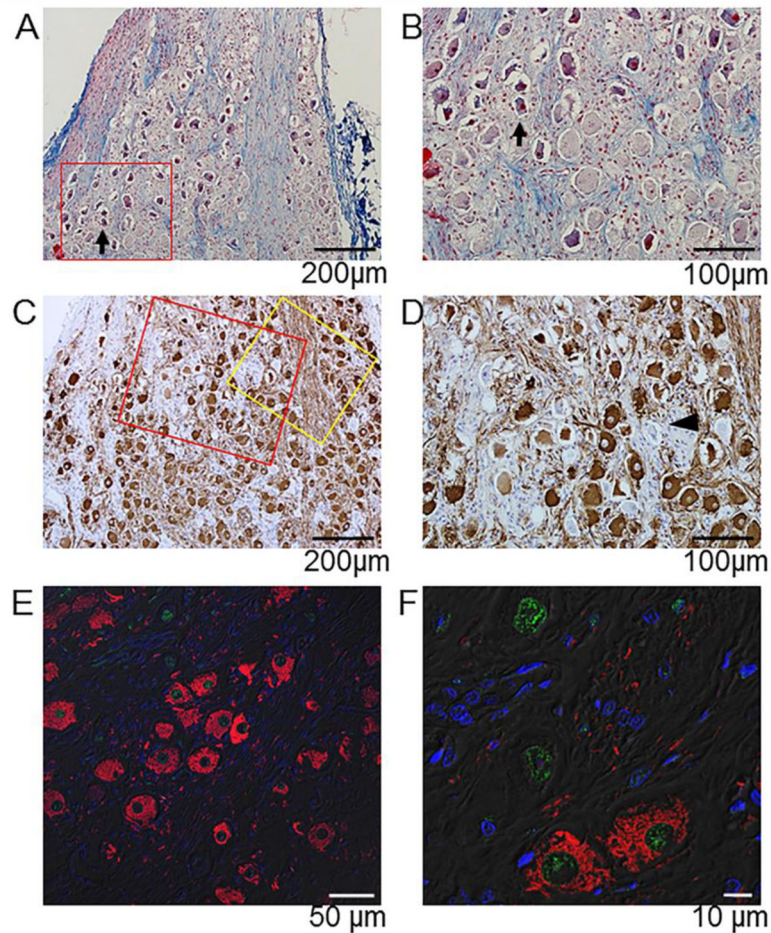
Figure 3. Histology of the LSG in a dog with bilateral RD

A shows Masson's trichrome staining of the SG. There were multiple injured ganglion cells characterized by pyknotic nuclei and contracted cytoplasm. **B** shows a high magnification view of the red box area in A. **C** shows TH staining. Multiple TH-negative ganglion cells were present. **D** shows a high magnification view of the area marked by a red box in **C**. An arrowhead points to a ganglion cell that stained negative for TH. **E** is a confocal image of the same LSG with TUNEL and TH double staining from the area marked by a yellow box area in **C**. Green indicates positive TUNEL stain while red indicates positive TH stain. Blue indicates positive DAPI staining of the nuclei. Several TUNEL positive ganglion cells were observed. Those cells had pyknotic cytoplasm and stained negative for TH, compatible with the findings in **C**. **F** shows the zoom-in view of E. There were four TUNEL positive cells, including two that stained negative and two stained positive for TH. The magnification of panels A–F were 100X, 200X, 100X, 200X, 400X and 800X, respectively. DAPI = 4′,6-diamidino-2-phenylindole; LSG = left stellate ganglion; SG = stellate ganglion; TH = tyrosine hydroxylase; TUNEL = terminal deoxynucleotidyl transferase dUTP nick end labeling.
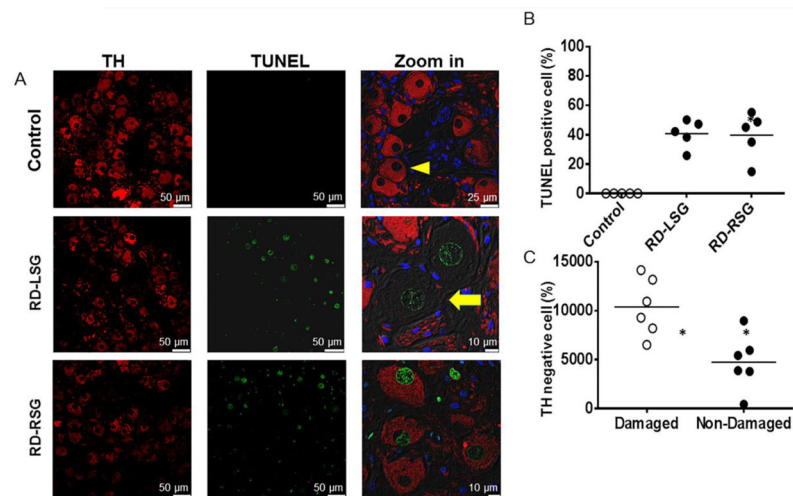
Figure 4. TH and TUNEL double staining of both SG

A shows confocal microscope images of TH and TUNEL double staining of the LSG of a control dog, the LSG of a RD dog (RD-LSG) and the RSG of a RD dog (RD-RSG). Green shows positive TUNEL stain, red indicates the positive TH stain and blue is the DAPI stain of the nuclei. The control ganglion cells were mostly TH-positive (yellow arrowhead in Control) and never TUNEL-positive. The TUNEL-positive ganglion cells might be stained either positive or negative for TH (yellow arrowhead in RD-LSG). **B** shows the percentage of TUNEL-positive ganglion cells in different groups of dogs. The TUNEL-positive ganglion cells were present in RD dogs but not in control dogs. There were no differences of percent TUNEL-positive cells between RSG and LSG in RD dogs. **C** shows the percentage of TH-negative ganglion cells in different groups of dogs. The TH-negative ganglion cells significantly increased in both SG in RD dogs as compared with control. There were no differences of percent TH-negative cells between RSG and LSG in RD dogs. * $p < 0.05$ compared with control by Wilcoxon rank-sum test. DAPI = 4′,6-diamidino-2-phenylindole; LSG = left stellate ganglion; RD = renal sympathetic denervation; RSG = right stellate ganglion; SG = stellate ganglion; TH = tyrosine hydroxylase; TUNEL = terminal deoxynucleotidyl transferase dUTP nick end labeling.
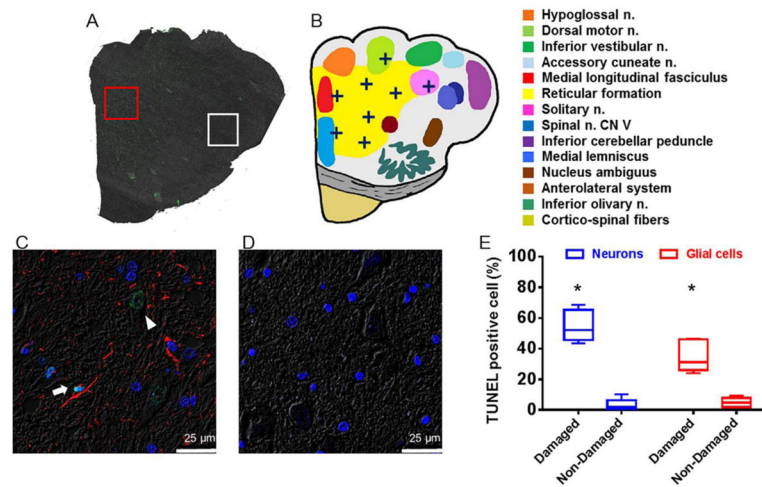
Figure 5. Immunofluorescence microscopy images of the brain stem at L1 in a bilateral RD dog
A shows confocal microscope image of TUNEL staining of the entire left half of the brain stem by combining images taken with 10X objective. The TUNEL positivity (green) was mostly distributed in the medial half of the brain stem. **B** shows a schematic of TUNEL positivity (dark blue cross) in different color-coded structures. **C** shows the TUNEL and GFAP double staining in high TUNEL-positivity area of Panel **A** (red box). Green indicates positive TUNEL stain, red indicates positive GFAP stain and blue is the DAPI stain of the nuclei. An arrowhead points to a TUNEL-positive neuron while an arrow points to a TUNEL-positive glial cell. There was high level of glial reaction as indicated by the strongly positive GFAP staining. **D** shows the same staining of the white box area in panel A. There were no TUNEL-positive or GFAP-positive cells in that region. Panel **E** shows the percentage of TUNEL-positive neurons and glial cells in "damaged zone" and "non-damaged zone" in bilateral RD dogs. The percentage of TUNEL-positive neuron and glial cells significantly increased in "damaged zone". (Panel A = scanning and merging of 100X images; Panel C and D = 800X). * $p < 0.05$ compared with non-damaged zone by Wilcoxon Signed Ranks Test. DAPI = 4′,6-diamidino-2-phenylindole; GFAP = glial fibrillary acid protein; L1 = level 1; RD = renal sympathetic denervation; TUNEL = terminal deoxynucleotidyl transferase dUTP nick end labeling.
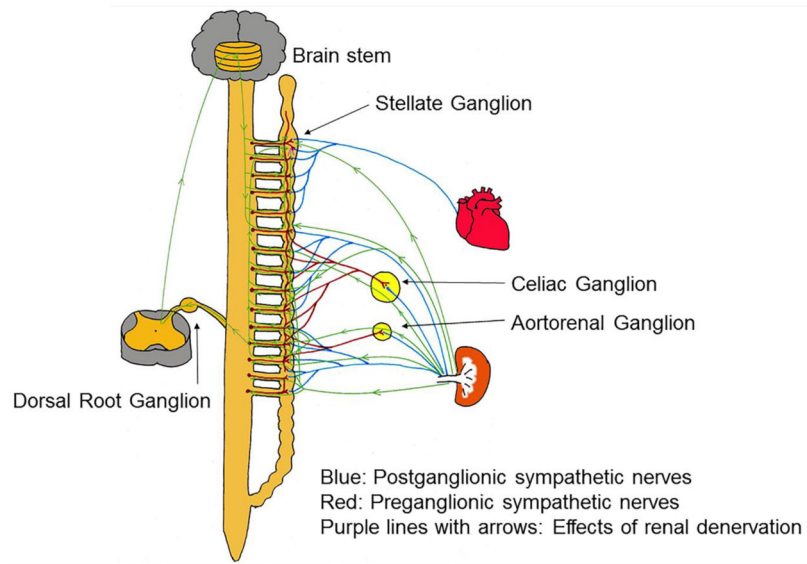
Figure 6. Schematics of possible connections among different nerve structures
There are multiple pathways to connect renal sympathetic nerves with the stellate ganglion.
Both preganglionic and postganglionic sympathetic fibers may innervate the renal artery.

Table 1

Effects of renal sympathetic denervation on nerve activities, RR interval and blood pressure.

	Baseline	1M after RD	2M after RD
aSGNA (μV)	14.0 ± 4.0	9.4 ± 2.8[*]	9.6 ± 2.0[*]
aVNA (μV)	12.6 ± 5.0	8.2 ± 2.6	8.0 ± 1.8
aSGNA/iVNA	1.32 ± 0.43	1.29 ± 0.38	1.38 ± 0.55
RR interval (ms)	778 ± 54	746 ± 63	786 ± 79
SBP (mmHg)	121 ± 9	115 ± 6	117 ± 8
DBP (mmHg)	81 ± 9	78 ± 7	80 ± 7

1M = one month; 2M = two months; DBP = diastolic blood pressure; aSGNA = average stellate ganglion nerve activity; aVNA = average vagal nerve activity; RD = renal sympathetic denervation; SBP = systolic blood pressure.

[*] p< 0.05 compared with baseline (Wilcoxon Signed Ranks test)